JREE: Vol. 9, No. 2, (Spring 2022) 59-74

Journal of Renewable Energy and Environment

Journal Homepage: www.jree.ir

Materials and Energy Research Center

MERC

Research Article

Reduction of Low Frequency Oscillations Using an Enhanced Power System Stabilizer via Linear Parameter Varying Approach

Vahid Nazari, Mohammad Hossein Mousavi, Hassan Moradi CheshmehBeigi *

Department of Electrical Engineering, Faculty of Engineering, Razi University, P. O. Box: 67144-14971, Kermanshah, Kermanshah, Iran.

PAPER INFO

Paper history:
Received: 27 September 2021
Revised in revised form: 23 December 2021
Scientific Accepted: 15 December 2021
Published: 12 April 2022

Keywords:
Power System Stabilizer,
Single Machine Infinite Bus Power System,
Linear Parameter Varying (LPV),
Linear Matrix Inequality (LMI)

ABSTRACT

Over the past decades, power engineers have begun to connect power grids to other networks such as microgrids associated with renewable units using long transmission lines to provide higher reliability and greater efficiency in production and distribution besides saving resources. However, many dynamic problems such as low frequency oscillations were observed as a result of these connections. Low frequency oscillation is a normal phenomenon in most power systems that causes perturbations and, thus, the grid stability and damping process are of paramount importance. In this paper, to attenuate these oscillations, a novel method for designing Power System Stabilizer (PSS) is presented via Linear Parameter-Varying (LPV) approach for a Single Machine Infinite Bus system (SMIB). Because the system under study is subject to frequent load and production changes, designing the stabilizer based on the nominal model may not yield the desired performance. To guarantee the flexibility of the stabilizer with respect to the aforementioned issues, the power system polytopic representation is used. In order to apply the new method, the nonlinear equations of the system at each operating point, located in a polytope, are parametrically linearized by scheduling variables. Scheduling variables can be measured online in any operating point. By using this model and following the H_∞ synthesis, feedback theories, and Linear Matrix Inequalities (LMIs), LPV controllers at all operating points are obtained. Finally, the simulation results verify the effectiveness of the proposed controller over classic and robust controllers with regard to uncertainties and changes in system conditions.

https://doi.org/10.30501/jree.2021.306909.1265

1. INTRODUCTION

Improving the stability of the power systems is one of the main goals, tasks, and aspirations of power engineers that has been of great significance in the last decades. The development of power grids, their diversity, and intertwining with renewable energies have brought about spontaneous low-frequency oscillations. Small and sudden disturbances in the grid cause natural fluctuations in the system. In the normal case, these oscillations die out rapidly and the amplitude of the oscillations does not exceed a certain amount. However, these fluctuations may continue for a long time and at worst, their amplitudes increase. Such fluctuations in the grid pose serious risks, making it difficult to exploit the system optimally. Various experiences of interconnected power systems indicate that these oscillations are caused by the excitation of electric modes of synchronous generators. Today, power system stabilizers are widely used to robustly improve the stability and overcome the perturbations [1-4].

*Corresponding Author's Email: ha.moradi@razi.ac.ir (H. Moradi CheshmehBeigi)
URL: https://www.jree.ir/article_148013.html

Several methods have been proposed in the literature to attenuate the low frequency oscillations of power systems. Planning a control strategy is essential to damping electromechanical oscillations while designing and creating a power system. Classic control systems, robust, adaptive, optimal, H_∞, fuzzy control-based methods, artificial neural networks, and a wide variety of optimization and artificial intelligence algorithms are some of the methods that have been developed in the field of stability and PSS design over the last years [5-10]. Utilizing fuzzy logic controller for designing a power system stabilizer was studied in an SMIB [11], showing the better performance of Fuzzy PSS (FPSS) over Classic PSS (CPSS) by considering the triangular and Gaussian functions to synthetize the controller. In [12], a predictive optimal adaptive PSS was presented for an SMIB. The simulation results of this optimization algorithm illustrated that the proposed POA-PSS method had preferable performance compared to CPSS. Another research was conducted to evaluate the output performance of CPSS and PID-PSS, which were optimized by Firefly and Bat algorithms. The results clarified that although CPSS with bat algorithm exhibited weak performance, the robust PID-PSS using firefly algorithm optimization could stabilize the proposed SMIB system for all operating conditions [13].

Please cite this article as: Nazari, V., Mousavi, M.H. and Moradi CheshmehBeigi, H., "Reduction of low frequency oscillations using an enhanced power system stabilizer via linear parameter varying approach", ***Journal of Renewable Energy and Environment (JREE)***, Vol. 9, No. 2, (2022), 59-74. (https://doi.org/10.30501/jree.2021.306909.1265).

Under [14] study, a stochastic metaheuristic population-based optimization algorithm named Sine Cosine Algorithm (SCA) was used for tuning PSS parameters. The research revealed that this technique was much more effective than other methods in exploration and exploitation to determine PSS parameters and improve the stability of a single machine connected to a large power system. An artificial intelligence method known as Ant Colony was employed to optimize a PID-PSS for an SMIB system. It was shown that the proposed control approach worked properly and the minimum overshoot for the frequency response and rotor angle were achieved [15].

In further studies, several methods have also been presented for multi-machine power systems. In [16], the design of PSS using the root locus method was investigated. The technique could be applied directly to the power systems and provided clear indication of damping degrees for various combination of PSS parameters. The result of this research indicated that the perturbations caused by noise input could be suppressed by the root locus-based PSS structure. In another study, the design of a fixed parameter PSS for synchronous performance in a multi-machine power system was executed. The stabilizer was designed to compensate for the transfer function. It was shown that the transfer function remained relatively constant over all working points. It was concluded that when facing disturbances, the PSS transfer function and dc gains were selected in a way that the phase and gain errors around the modal frequencies were kept to a minimum. [17]. In [18], a new evolutionary algorithm-based approach was proposed to perfectly design multi-machine power system stabilizers. The presented method used the Particle Swarm Optimization (PSO) algorithm to search for optimal settings of PSS parameters. Two objective functions based on eigenvalues were considered to increase the attenuation of the electromechanical modes of the system. Robustness of the proposed method also depended on the initial guess, which is considered as its drawback. Thus, the simulation results were analyzed to guarantee the desired performance of the proposed PSS in the presence of various perturbations and loading issues. It was demonstrated that the novel Modified PSO algorithm presented in the paper brought about some advantages compared to previous PSO approaches. Further research was conducted to design a PSS for the multi-machine power system using the output feedback sliding mode control technique. The nonlinear model of the multi-machine power system was linearized at different operating points. The slide signal was taken as output and the output feedback sliding mode control was applied at an appropriate sampling rate. This method did not require complete states feedback and was easy to implement [19]. The main result of this research is that the proposed controller can damp the oscillations much faster than the classical PSS, which increases the responsiveness of the control system. In [20], an adaptive fuzzy control method was employed to form a decentralized load frequency controller in a two-zone interconnected power system. The Adaptive Fuzzy Load Frequency Controller (AFLFC) was implemented to enhance the frequency dynamic performance and transmitted power through the transmission lines during sudden load changes. The results illustrated that this method provided good attenuation control and reduced the frequency deviation overshoot in both regions. Gray Wolf Optimization (GWO) algorithm was tested to create a Wide-Area Power System Stabilizer (WAPSS) and it was examined in some multi-machine power systems. It was observed that the proposed strategy came with a multitude number of advantages such as damping the inter-area oscillations and compensating the detrimental effects of communication delays [21]. In [22], an optimal Model Reference Adaptive System (MRAS) was addressed to devise an effective PSS utilizing in multi-machine power systems. Through the suggested strategy in this research, the speed profile of the generator was enhanced and much more damping torque was provided upon injecting the stabilizing signals to the excitation part of the control system. The robust approach has also been of interest to researchers in recent years due to its impacts on improving system performance. One novel research investigated a robust strategy for a single machine infinite linked to a static synchronous compensator (STATCOM). The purpose of employing STATCOM was to regulate voltage and lessen the fluctuations via NSGII algorithm. The proposed system acts like a PSS to deal with disturbances. There were three scenarios considering PID controllers for speed loop, voltage loop, and both. The results illustrated that the third scenario positively affected the damping degree for both speed and voltage control aims [23]. It was shown in [24] that a robust power system stabilizer for enhancement of stability in power system ensured better performance in comparison with the conventional fuzzy-PID controller. The methods mentioned in this section for designing and tuning power system stabilizers present many drawbacks. In addition to the random selection of the initial population, local entrapment and inopportune convergence are among the disadvantageous of heuristic algorithms. Then, meta-heuristic algorithms have been introduced to compensate earlier issues. Some other studies have focused on linear parameter varying to achieve good performance for power system stabilizers. A Least Mean Square (LMS) method was used as an LPV identification algorithm in [25]. This algorithm was composed of the LPV model based on the interpolation of m linear local models and active and reactive power were considered as scheduling parameters. The simulation and experimental test showed that the applied methodology had a desirable damping effect on electromechanical oscillating terms. Also, another LPV system identification methodology was presented in [26]. Principal Component Analysis-based (PCA-based) parameter set mapping was employed to decrease the number of models and create a simpler LPV model. In this way, the computational burden of the modeling strategy was reduced. The suggested LPV controller verified the suppressing features and damping properties against fluctuations, especially in multi-machine power systems facing different operating conditions. Despite the relatively good performances of different systems, a strong mathematical basis is not included and even much time may be spent for solving optimization problems. Also, getting an accurate response due to the complexity of the systems could be difficult to reach. Additionally, the proposed robust PSS and CPSS tested in the literature mainly offer one simple controller for all operating points which cannot work under some uncertainties and system disturbances. On the other hand, an enhanced LPV-PSS presents separate controllers for the whole working points and uncertain circumstances. Online parameter tuning in LPV control systems is a major privilege amongst other controllers to adjust the PSS parameters due to unpredictable performances of a system. It is to be mentioned that proven control theories and lemmas support the LPV systems.

Linear Parameter Varying (LPV) modeling refers to linear dynamical models and the description of their state space depends on an exogenous variable parameter. In these models, the exogenous parameter operates independently and the state space model is dependent on it, that is, the exogenous parameter changes are independent of the system and a unique linear state space model is defined for each parameter. Exogenous parameters are called scheduling parameters. LPV models have a profound relationship with gain-scheduling strategies which is, in fact, the extension of the classical gain-scheduling method. The only difference is that in gain-scheduling models, unlike LPV models, the free parameter is endogenous, meaning that it originates within the system. The basis of both theories is to parse a nonlinear controller and create a set of linear controllers for a nonlinear system [27-28].

The main purpose of this paper is to design a power system stabilizer using LPV control method which is used to enhance the oscillations' damping of a single-machine power system connected to an infinite bus in a wide range of operating conditions. In order to apply this new technique, the nonlinear equations of the system at any operating points in a polytopic space are parameterized linearly by setting online-measured parameters. Next, the search space is reduced from a non-convex space to a convex sub-space to solve the optimization problem. Considering H_∞ algorithm and optimization LMIs, the LPV controller is designed using output and state feedback theories. This way, contrary to the pre-mentioned controllers, there would be a controller for every single working point in the determined polytopic space. Hence, by taking online feedbacks, the PSS parameters can be tuned uniquely. In other words, by proceeding from one working point to another, the controller model also changes accordingly. This empowers the control system to perfectly perform during different conditions.This article is organized as follows. Introduction is presented in Section 1. In Section 2, preliminaries are introduced. In Section 3, the LPV modeling of Single Machine Infinite Bus Power System with polytopic representation is stated. Simulation and results are given in Section 4. Conclusion is discussed in Section 5.

2. PRELIMINARIES

2.1. LPV systems

The LPV model is a dynamic linear state space model. Although the matrices of this model are not specific, they depend on the system free parameter. The general form of such a model is as follows:

$$\begin{aligned}\dot{x} &= A(\theta)x + B(\theta)u\\ y &= C(\theta)x\end{aligned} \tag{1}$$

where θ is an exogenous parameter that can be time dependent; u and y are input and output. As can be seen, this is a typical representation of the state space. One thing to note is that within a given timeframe, the parameter can cross any arbitrary path whose quality is generally out of the system control. It is also worth mentioning that there are bounds on magnitude and rate of variation for exogenous parameters [27].

For all $t \geq 0$,

$$\begin{aligned}-\mu \leq \theta(t) \leq \mu\\ -\rho \leq \dot{\theta}(t) \leq \rho\end{aligned} \tag{2}$$

2.2. Output feedback LPV controller design

By expanding (1), the state space complete model of the LPV system is obtained as follows:

$$G(\theta):\begin{cases}\dot{x} = A(\theta)x + B_1(\theta)w + B_2u\\ z = C_1(\theta)x + D_{11}(\theta)w + D_{12}(\theta)u\\ y = C_2(\theta)x + D_{21}(\theta)w\end{cases} \tag{3}$$

where z is performance output, y sensed output, u control input, and w represents disturbance input. The state space model of the full-order output feedback controller is defined as follows:

$$K(\theta):\begin{cases}\dot{x}_k = A_K(\theta)x_K + B_K(\theta)y\\ u = C_K(\theta)x_K + D_K(\theta)y\end{cases} \tag{4}$$

The closed loop system consisting of plant (P) and output feedback controller (K) defined in (3) and (4) is expressed as follows:

$$H(\theta):\begin{cases}\dot{x}_{cl} = A_{cl}(\theta)x_{cl} + B_{cl}(\theta)w\\ z = C_{cl}(\theta)x_{cl} + D_{cl}(\theta)w\end{cases} \tag{5}$$

The generilized separate form is considered as follows:

$$\begin{pmatrix}A_{cl} & B_{cl}\\ C_{cl} & D_{cl}\end{pmatrix} = \begin{pmatrix}A + BD_KC & BC_K & B_w + BD_KD_w\\ B_KC & A_K & B_KD_w\\ C_z + D_zD_KC & D_zC_K & D_{zw} + D_zD_KD_w\end{pmatrix} \tag{6}$$

Figure 1 presents the block diagram of the closed loop system in the output feedback design.

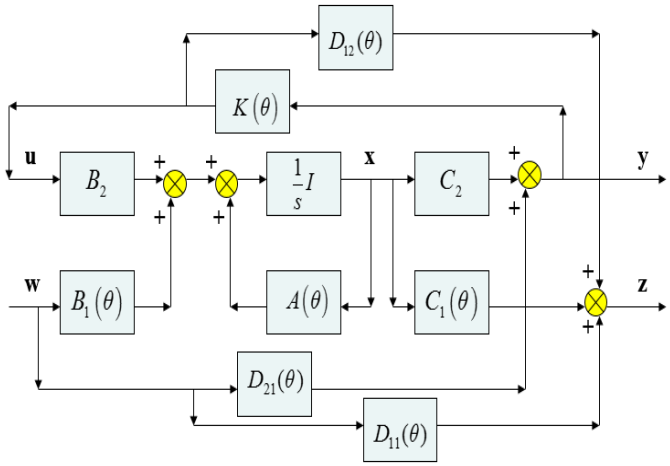

Figure 1. Block diagram of closed loop system in output feedback method

2.2.1. H_∞ based output feedback controller considering Single Quadratic Lyapunov Function (SQLF)

In this case, the variation rate of exogenous parameters is considered as desired. This method is stated through two approaches. The purpose to review these two perspectives is to figure out which one exhibits better performance and accuracy.

Theorem 1. If for a positive value of γ_∞, there will be a definite positive matrix of $X, Z \in S^n$ and the matrices of the dependent parameter $A_K(\theta) \in R^{n\times n}$, $B_K(\theta) \in R^{n\times n_y}$, $C_K(\theta) \in R^{n_u\times n}$, $D_K(\theta) \in R^{n_u\times n_y}$, respectively, so that the LMIs (7) and (8) are satisfied simultaneously, then the closed loop system $H(\theta)$ in (5) is exponentially stable and the constraint (norm) H_∞ of transfer function from disturbance input w to

performance output z in the closed loop system $H(\theta)$ becomes smaller than γ_∞ in (9) [29]. Therefore, the state space matrices of controller $K(\theta)$ can be obtained from Equation (10).

$$\Upsilon_\infty(\theta)=\begin{pmatrix}\mathrm{He}\left\{\begin{pmatrix}A(\theta)X+B_2C_K(\theta) & A(\theta)B_2D_K(\theta)C_2\\ A_K(\theta) & ZA(\theta)+B_K(\theta)C_2\end{pmatrix}\right\} & * & \begin{bmatrix}B_1(\theta)+B_2D_K(\theta)D_{21}\\ ZB_1(\theta)+B_K(\theta)D_{21}\end{bmatrix}\\ \begin{bmatrix}C_1(\theta)X+D_{12}C_K(\theta) & C_1(\theta)+D_{12}D_K(\theta)C_2\end{bmatrix} & -\gamma_\infty I_{nz} & D_{11}(\theta)+D_{12}D_K(\theta)D_{21}\\ * & * & -\gamma_\infty I_{nw}\end{pmatrix}<0 \tag{7}$$

The parameters used in the above LMI are state, input, and output matrices, which were introduced in Section 2.2. By solving this LMI, the controller matrices are obtained.

$$\begin{pmatrix}X & I_n\\ I_n & Z\end{pmatrix}>0 \tag{8}$$

$$\sup_{w\in L_2, w\neq 0}\frac{\|z\|_2}{\|w\|_2}<\gamma_\infty \tag{9}$$

$$\begin{cases}A_K(\theta)=Z^{-1}(ZA(\theta)X+ZB_2C_K(\theta)-A_K(\theta)\\ -\left(ZB_2D_K(\theta)-B_K(\theta)\right)C_2X)Y^{-1}\\ B_K(\theta)=Z^{-1}\left(ZB_2D_K(\theta)-B_K(\theta)\right)\\ C_K(\theta)=(C_K(\theta)-D_K(\theta)C_2X)Y^{-1}\\ D_K(\theta)=D_K(\theta)\end{cases} \tag{10}$$

where

$$Y=X-Z^{-1} \tag{11}$$

Theorem 2. For any given value of λ, the closed loop system consisting of the system (3) and the LPV controller is stable by displaying the given state space in (4) if and only if there are constant decision matrices $P_1\in R^{n\times n}$, $P_2\in R^{n\times n}$, $P_3\in R^{n\times n}$, and $Y\in R^{n\times n}$, as well as the dependent parameters $L_1(\theta)\in R^{n\times n}$, $L_2(\theta)\in R^{n\times r}$, $L_3(\theta)\in R^{p\times n}$ and $X(\theta)\in R^{n\times n}$, $S(\theta)\in R^{n\times n}$, so that Conditions (12) and (13) are satisfied simultaneously; then, the closed loop system $H(\theta)$ is exponentially stable in (5) and H_∞ norm of the transfer function from the disturbance input w to performance output z in the closed loop system $H(\theta)$ will be less than the value of γ_∞ in (16) [30]. Therefore, the state space matrices of the controller $K(\theta)$can be obtained from Equation (15):

$$\begin{pmatrix}P_1 & P_2\\ P_2' & P_3\end{pmatrix}>0 \tag{12}$$

$$\begin{pmatrix}\dot{P}_1-\mathrm{He}(A(\theta)X(\theta)+B_2(\theta)L_3(\theta)) & *\\ P_2'-L_1(\theta)-A'(\theta) & \dot{P}_3-\mathrm{He}(YA(\theta)+L_2(\theta)C_2(\theta))\\ -C_1(\theta)X(\theta)-D_2(\theta)L_3(\theta) & -C_1(\theta)\\ B_1' & B_1'(\theta)Y'+D_{21}'(\theta)L_2'(\theta)\\ X(\theta)-P_1-\lambda X'(\theta)A'(\theta)-\lambda L_3'(\theta)B_2'(\theta) & I-P_2-\lambda L_1'(\theta)\\ S(\theta)-P_2'-\lambda A'(\theta) & Y-P_3-\lambda A'(\theta)Y'-\lambda C_2'(\theta)L_2'(\theta)\end{pmatrix}$$
$$\begin{pmatrix}* & * & * & *\\ * & * & * & *\\ I & * & * & *\\ D_1'(\theta) & \gamma_\infty^2 I & * & *\\ -\lambda X'(\theta)C_1'(\theta)-\lambda L_3'(\theta)D_2'(\theta) & 0 & \lambda(\mathrm{He}(X(\theta))) & *\\ -\lambda C_1'(\theta) & 0 & \lambda S(\theta)+\lambda I & \lambda(\mathrm{He}(Y))\end{pmatrix}<0 \tag{13}$$

The output variables and the controller state space representation are achieved as follows:

$$\begin{cases}A_K(\theta)=V(L_1(\theta)-YA(\theta)X(\theta)-YB_2(\theta)L_3(\theta)-L_2(\theta)C_2(\theta)X(\theta))\\ B_K(\theta)=V\left(L_2(\theta)-YB_2(\theta)\right)\\ C_K(\theta)=L_3(\theta)\\ D_K(\theta)=0\\ \varepsilon_K(\theta)=V\left(S(\theta)-YX(\theta)\right)\end{cases} \tag{14}$$

where

$$\begin{cases}A_K(\theta)=A_K(\theta)\varepsilon_K^{-1}(\theta)\\ B_K(\theta)=B_K(\theta)\\ C_K(\theta)=C_K(\theta)\varepsilon_K^{-1}(\theta)\\ D_K(\theta)=D_K(\theta)\end{cases} \tag{15}$$

$$\|H_{zw}\|_\infty^2=\sup_{\|w(k)\|_2\neq 0}\frac{\|z(k)\|_2^2}{\|w(k)\|_2^2}<\gamma_\infty^2 \tag{16}$$

Matrix V is opted as desired, which can be an identity matrix with the appropriate dimension [30]. It should be noted that according to Theorem 2, various stabilizer controllers can be designed by selecting each different λ.

2.2.2. H∞ based output feedback controller considering Parameter Dependent Lyapunov Function (PDLF)

In this case, the variation rate of exogenous parameters is considered slow.

Theorem 3. For any given value of λ, the closed loop system consisting of the system (3) and the LPV controller is stable with the state space represntation in (4) if and only if there are symmetric dependent parameter $P_1\in R^{n\times n}$, $P_3\in R^{n\times n}$ and the dependent matrix parameters of $L_1(\theta)\in R^{n\times n}$, $L_2(\theta)\in R^{n\times r}$, $L_3(\theta)\in R^{p\times n}$ and $P_2\in R^{n\times n}$, $X(\theta)\in R^{n\times n}$, $S(\theta)\in R^{n\times n}$ and the constant decision matrix $Y\in R^{n\times n}$ so that the Conditions (17) and (18) are satisfied simultaneously. Then, the closed loop system $H(\theta)$ in (5) is exponentially stable and the H_∞ norm of the transfer function from disturbance input w to performance output z in the close loop system $H(\theta)$ will be smaller than the value of γ_∞ in (21). Therefore, the controller state space matrices $K(\theta)$ can be calculated from Equation (20) as follows [30]:

$$\begin{pmatrix}P_1(\theta) & P_2(\theta)\\ P_2'(\theta) & P_3(\theta)\end{pmatrix}>0 \tag{17}$$

$$\begin{pmatrix}\dot{P}_1(\theta)-\mathrm{He}(A(\theta)X(\theta)+B_2(\theta)L_3(\theta)) & *\\ P_2'(\theta)-L_1(\theta)-A'(\theta) & \dot{P}_3(\theta)-\mathrm{He}(YA(\theta)+L_2(\theta)C_2(\theta))\\ -C_1(\theta)X(\theta)-D_2(\theta)L_3(\theta) & -C_1(\theta)\\ B_1' & B_1'(\theta)Y'+D_{21}'(\theta)L_2'(\theta)\\ X(\theta)-P_1(\theta)-\lambda X'(\theta)A'(\theta)-\lambda L_3'(\theta)B_2'(\theta) & I-P_2(\theta)-\lambda L_1'(\theta)\\ S(\theta)-P_2'(\theta)-\lambda A'(\theta) & Y-P_3(\theta)-\lambda A'(\theta)Y'-\lambda C_2'(\theta)L_2'(\theta)\end{pmatrix}$$
$$\begin{pmatrix}* & * & * & *\\ * & * & * & *\\ I & * & * & *\\ D_1'(\theta) & \gamma_\infty^2 I & * & *\\ -\lambda X'(\theta)C_1'(\theta)-\lambda L_3'(\theta)D_2'(\theta) & 0 & \lambda(\mathrm{He}(X(\theta))) & *\\ -\lambda C_1'(\theta) & 0 & \lambda S(\theta)+\lambda I & \lambda(\mathrm{He}(Y))\end{pmatrix}<0 \tag{18}$$

The output variables and the controller state space reprentation are obtained as follows:

$$\begin{pmatrix}* & * & * & *\\ * & * & * & *\\ I & * & * & *\\ D_1'(\theta) & \gamma_\infty^2 I & * & *\\ -\lambda X'(\theta)C_1'(\theta)-\lambda L_3'(\theta)D_2'(\theta) & 0 & \lambda(\mathrm{He}(X(\theta))) & *\\ -\lambda C_1'(\theta) & 0 & \lambda S(\theta)+\lambda I & \lambda(\mathrm{He}(Y))\end{pmatrix}<0 \tag{19}$$

where

$$\begin{cases} A_K(\theta) = A_K(\theta)\varepsilon_K^{-1}(\theta) \\ B_K(\theta) = B_K(\theta) \\ C_K(\theta) = C_K(\theta)\varepsilon_K^{-1}(\theta) \\ D_K(\theta) = D_K(\theta) \end{cases} \quad (20)$$

$$\|H_{zw}\|_\infty^2 = \sup_{\|w(k)\|_2 \neq 0} \frac{\|z(k)\|_2^2}{\|w(k)\|_2^2} < \gamma_\infty^2 \quad (21)$$

Matrix V is opted as desired, which can be an identity matrix with the appropriate dimension [30]. It should be noted that according to Theorem 3, various stabilizer controllers can be designed by selecting each different λ.

2.3. State feedback LPV controller design

Theorem 4. If in the following optimization problem, for a positive ρ, there are positive and definite matrices $X(\theta)$ and $W(\theta)$ so that the LMI Condition in (22) for the system (3) can be satisfied, then the closed loop system $T(\theta)$ in (20) is stable and the norm of the closed loop (23) is met [31].

$$\begin{pmatrix} A(\theta)X(\theta) + B_2W(\theta) + (A(\theta)X(\theta) + B_2W(\theta))^T & & \\ B_1^T(\theta) & & \\ C_1(\theta)X(\theta) + D_{12}(\theta)W(\theta) & & \end{pmatrix}$$

$$\begin{matrix} B_1(\theta) & (C_1(\theta)X(\theta) + D_{12}W(\theta)^T \\ -I & D_{11}^T(\theta) \\ D_{11}(\theta) & -\rho I \end{matrix} \Bigg) < 0 \quad (22)$$

where $X(\theta), W(\theta) > 0$.

$$\|T_{wz}\|_\infty < \sqrt{\rho} \quad (23)$$

Then, the state feedback controller gain can be expressed through the following equation [30]:

$$K(\theta) = W(\theta) \times X^{-1}(\theta) \quad (24)$$

$$T(\theta): \begin{cases} \dot{x}_{cl} = A_{cl}(\theta)x_{cl} + B_{cl}(\theta)w \\ z = C_{cl}(\theta)x_{cl} \end{cases} \quad (25)$$

Figure 2 demonstrates the block diagram of the closed loop system in the state feedback design method.

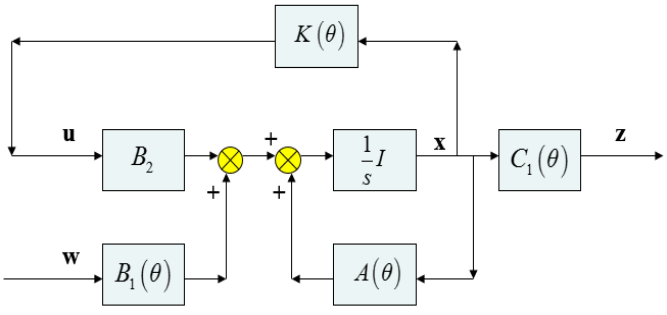

Figure 2. Block diagram of the closed loop system in state feedback method

In designing a controller using this technique, much progress has been made beyond stabilization (as minimum expectation of the controller), especially in the discussion of disturbances from LPV systems and minimization of inductive norms, improvements are significant [27]. It is to be noted that in most robust control topics, achieving a desirable function leads to minimization of inductive norm of a weighted function and progress in minimizing these norms provides progress in obtaining the desired system performance.

3. PROPOSED LPV MODELING of SINGLE MACHINE INFINTE BUS POWER SYSTEM

The system under study is a single machine infinite bus power system connecting via a transmission line. This system is represented by a fourth-order linear model [32]. The block diagram of this model is shown in Figure 3 below.

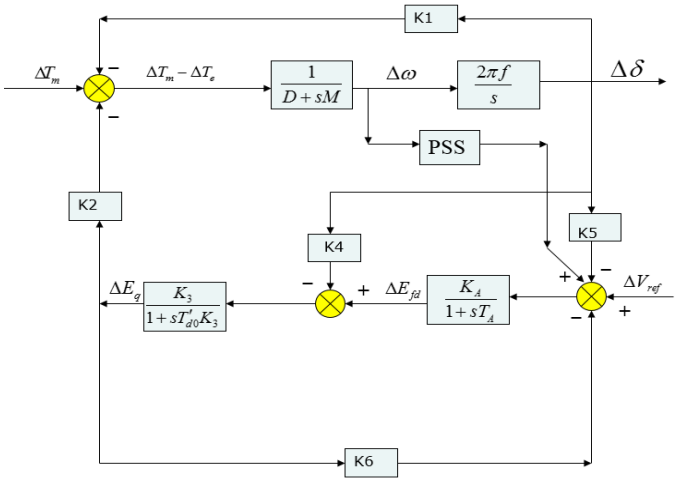

Figure 3. Mathematical model of the single machine infinite bus power system

In the proposed LPV modeling, to ensure the flexibility of the PSS, a polytopic representation of the power system is employed. As is clear from Fig. 3, $(k_1, k_2, k_3, k_4, k_5, k_6)$ are fourth-order model constants that remain dependent on the loading conditions of the active power (P), the reactive power (Q), and the external reactance of transmission line (x_e).

Mathematical equations concerned with how to convert $k_1 \dots k_6$ to P, Q, x_e were given in reference [33, 34]. In fact, Parameters $k_1 \dots k_6$ are obtained via linearized small perturbation relations of a single generator supplying an infinite bus through external impedance. In other words, the proposed model $k_1 \dots k_6$ emerges from the relationship between the concept of small perturbation analysis and synchronous generator elements [38]. The proposed working points (P Q x_e) are per unit values which are arbitrarily determined from the specified intervals for each of the parameters. The LPV model of a single machine infinite bus power system can be written as follows:

$$G(\theta): \begin{cases} \dot{x} = A(k_p)x + B_w w + B_u u \\ z = C_z x + D_z u \\ y = C_y x \end{cases} \quad (26)$$

z, w and y are stabilizer output, the disturbance input, and the measured output, respectively. Here, the velocity change $\Delta\omega$ is considered as the measured output. Disturbance input can be selected as a change in the mechanical torque input or a change in the voltage reference. The state vector $x \in R^4$ is defined as $x = [\Delta\delta \quad \Delta\omega \quad \Delta E_q \quad \Delta E_{fd}]$, where $\Delta\delta$, ΔE_q, and ΔE_{fd} are load angle deviation, induced electromagnetic force deviation corresponding to the field current, and deviation in the generator field excitation voltage. The matrices for representing the state space are as follows [32].

$$(k_p)=\begin{pmatrix} 0 & \omega_0 & 0 & 0 \\ \frac{-k_1}{M} & \frac{-D}{M} & \frac{-k_2}{M} & 0 \\ \frac{-k_4}{T'_{d0}} & 0 & \frac{-1}{T'_{d0}k_3} & \frac{1}{T'_{d0}} \\ \frac{-K_E k_5}{T_E} & 0 & \frac{-K_E k_6}{T_E} & \frac{-1}{T_E} \end{pmatrix}, B_u=\begin{pmatrix} 0 \\ 0 \\ 0 \\ \frac{K_E}{T_E} \end{pmatrix}$$

$$B_w=\begin{pmatrix} 0 \\ \frac{1}{M} \\ 0 \\ 0 \end{pmatrix}, C_y=(0 \quad 1 \quad 1 \quad 1) \tag{27}$$

where T_E, K_E, T'_{d0} and M are exciter time constant, exciter gain, open circuit field time constant, and inertia coeficient, respectively.

Note: $C_1=C_z$ and $C_2=C_y$ may be selected as $C_z=C_y$ and also $D_z=0$. Doing this, the H_∞ norm of the closed loop system is reduced from the input w to z as well as the effect of external disturbance on the output performance. Based on the analysis performed in [33], k_4 can be written as $(x_d-x'_d)k_2$, in which x_d and x'_d are the d-axis synchronous reactance and the d-axis transient reactance, respectively. In addition, it can be written in the matrix (27):

$$k_{3i}=\frac{1}{k_3} \tag{28}$$

Therefore, system matrices can be expressed as follows:

$$(k_p)=\begin{pmatrix} 0 & \omega_0 & 0 & 0 \\ \frac{-k_1}{M} & 0 & \frac{-k_2}{M} & 0 \\ \frac{-(x_d-x'_d)k_2}{T'_{d0}} & 0 & \frac{-k_{3i}}{T'_{d0}} & \frac{1}{T'_{d0}} \\ \frac{-K_E k_5}{T_E} & 0 & \frac{-K_E k_6}{T_E} & \frac{1}{T_E} \end{pmatrix}, B_u=\begin{pmatrix} 0 \\ 0 \\ 0 \\ \frac{K_E}{T_E} \end{pmatrix}$$

$$B_w=\begin{pmatrix} 0 \\ \frac{1}{M} \\ 0 \\ 0 \end{pmatrix}, C_y=(0 \quad 1 \quad 0 \quad 0) \tag{29}$$

$$A(k_p)=A_0+k_1A_1+k_2A_2+k_{3i}A_3+k_5A_5+k_6A_6 \tag{30}$$

In Equation (30), the system matrix $A(k_p)$ is written as an expression and separated by parameters and constant matrices A_0, A_1, A_2, A_3, A_5 and $A_6$where each parameter changes within a certain range:

$$\begin{cases} k_1 \in [k_1^-, k_1^+] \\ k_2 \in [k_2^-, k_2^+] \\ k_{3i} \in [k_{3i}^-, k_{3i}^+] \\ k_5 \in [k_5^-, k_5^+] \\ k_6 \in [k_6^-, k_6^+] \end{cases}$$

under different loading conditions.

$k_i^-(k_i^+)$ represent the boundries of the k_i parameter corresponding to the $P \in [P^-, P^+]$, $Q \in [Q^-, Q^+]$and $x_e \in [x_e^-, x_e^+]$ values. The affine parameter-dependent model in (30) can be converted to a olytopic model as (32). The parametric vector $k=[k_1 \quad k_2 \quad k_{3i} \quad k_5 \quad k_6]$ creates a 32-corner polytope whose corners are as follows:

$$\begin{cases} k_{cor32}=[k_1^- \quad k_2^+ \quad k_{3i}^+ \quad k_5^+ \quad k_6^+] \\ k_{cor32}=[k_1^+ \quad k_2^- \quad k_{3i}^+ \quad k_5^+ \quad k_6^+] \\ \qquad\qquad . \\ \qquad\qquad . \\ \qquad\qquad . \\ k_{cor32}=[k_1^- \quad k_2^- \quad k_{3i}^- \quad k_5^- \quad k_6^-] \end{cases} \tag{31}$$

For all $P \in [P^-, P^+]$, $Q \in [Q^-, Q^+]$ and $x_e \in [x_e^-, x_e^+]$ values, the system matrix can be obtained as:

$$A(k_p)=A(k) \in S := Co\{A_1, A_2, \dots, A_{32}\}:$$

$$=\left\{\sum_{i=1}^{i=32} a_i A_i : a_i \geq 0, \sum_{i=1}^{i=32} a_i = 1\right\} \tag{32}$$

where $A_1=A(k_{cor1}), A_2=A(k_{cor2}), \dots, A_{32}=A(k_{cor32})$.

In this study, the design of PSS using the output feedback and the state feedback method via LPV approach for optimal placement of poles in accordance with the working conditions $P \in [P^-, P^+]$, $Q \in [Q^-, Q^+]$ and $x_e \in [x_e^-, x_e^+]$ is presented so that the H_∞norm of the closed loop system can be minimized. Furthermore, the PSS transfer function is strictly proper and its order is equal to the system order (full order controller). The state space representation of PSS controller and closed loop system are shown in accordance with (4) and (5) as follows:

$$K(k_p): \begin{cases} \dot{x}_K = A_K(k_p)x_K + B_K(k_p)y \\ u = C_K(k_p)x_K + D_K(k_p)y \end{cases} \tag{33}$$

The closed loop system consists of a plant (29) and a controller (33), as obtained below:

$$T(k_p): \begin{cases} \dot{x}_{cl} = A_{cl}(k_p)x_{cl} + B_{cl}(k_p)w \\ z = C_{cl}(k_p)x_{cl} + D_{cl}(k_p)w \end{cases} \tag{34}$$

where

$$\begin{pmatrix} A_{cl} & B_{cl} \\ C_{cl} & D_{cl} \end{pmatrix}=\begin{pmatrix} A+BD_KC & BC_K & B_w+BD_KD_w \\ B_KC & A_K & B_KD_w \\ C_z+D_zD_KC & D_zC_K & D_{zw}+D_zD_KD_w \end{pmatrix} \tag{35}$$

4. SIMULATION AND RESULTS

In this section, by employing the mentioned Theorems and Equations, simulations are done according to the defined scenarios. Optimization problems are solved using the YALMIP [35] and ROLMIP [36] toolboxes runnig in MATLAB software. SeDuMi and SPDT3 are used as LMI solvers.

4.1. Output feedback structure

Theorems 1 and 2 of Section 2.2.1. are used for system (29) with a 32-corner polytope corresponding to the following parameters:

$P \in [P^-, P^+]$, $Q \in [Q^-, Q^+]$and $x_e \in [x_e^-, x_e^+]$

$$\begin{cases} k_1 \in [k_1^-, k_1^+] \\ k_2 \in [k_2^-, k_2^+] \\ k_{3i} \in [k_{3i}^-, k_{3i}^+] \\ k_5 \in [k_5^-, k_5^+] \\ k_6 \in [k_6^-, k_6^+] \end{cases}$$

Finally, the control parameters of the output feedback design are obtained using Equation (10) and (15).

Considering the single machine infinite bus power system and the 32 corners obtained from its polytopic representation, the LPV stabilizer design is addressed. In the simulations performed, the range of changes in machine parameters is considered as follows [32]:

$$\begin{array}{l} P \in [0.2 \quad 1] \text{ p.u} \\ Q \in [-0.2 \quad 0.5] \text{ p.u} \\ x_e \in [0.4 \quad 0.8] \text{ p.u} \end{array} \tag{36}$$

The parameters k_1 to k_6 will also change as shown in Appendix B, in the specific period $[k_i^-, k_i^+]$ as follows:

$$\begin{cases} [k_1^- \quad k_1^+] = [0.67027 \quad 1.7130] \\ [k_2^- \quad k_2^+] = [0.0377 \quad 1.3255] \\ [k_{3i}^- \quad k_{3i}^+] = [2.14285 \quad 2.77778] \\ [k_5^- \quad k_5^+] = [-0.13991 \quad 0.16554] \\ [k_6^- \quad k_6^+] = [0.3810 \quad 0.82008] \end{cases} \quad (37)$$

To investigate the effectiveness of the proposed method, the simulation results of the stabilizer designed by Theorems 1 and 2 in Section 2.2.1 and a classical stabilizer [37] as well as a H_∞ robust stabilizer [32] are compared.

H_∞ Robust output feedback PSS

$$\frac{76.74\times(1+0.287s)(1+0.648s)(1+0.0126s)}{(1+0.0205s)(1+0.0324s)(1\times10^{-5}s^2+2.35\times10^{-3}s+1)} \quad (38)$$

$$C_{pss} = \frac{K_s T_w s}{1+T_w s} \times \frac{(1+T_1 s)(1+T_3 s)}{(1+T_2 s)(1+T_4 s)} = \frac{14\times10s}{1+10s} \times \frac{(0.08s^2+0.65s+1)}{(0.0052s^2+0.14s+1)} \quad (39)$$

K_s is the PSS gain, T_w is the Washout time constant, and $T_1 \ldots T_4$ are the time constants of the lead compensators.

Here are the simulation results of a sudden change in the input mechanical torque, which indicates a short circuit at a particular moment and its elimination after a certain period of time that occurs in three modes of operation.

Table 1. Summary of the considered operating conditions

Operating conditions	Values
1st: Lag power factor	$P = 1, Q = 0.2, x_e = 0.4$
2nd: Lead power factor	$P = 1, Q = -0.2, x_e = 0.8$
3rd: Lag power factor	$P = 0.2, Q = 0.5, x_e = 0.4$
4th: Lead power factor	$P = 0.3, Q = -0.1, x_e = 0.6$

In this case, first, using Theorems 1 and 2 in Section 2.2.1, the Liapanov function is fixed and as a result, the dynamics of the system are considered to be relatively fast. The simulation results are obtained as follows (Figure4 - Figure14).

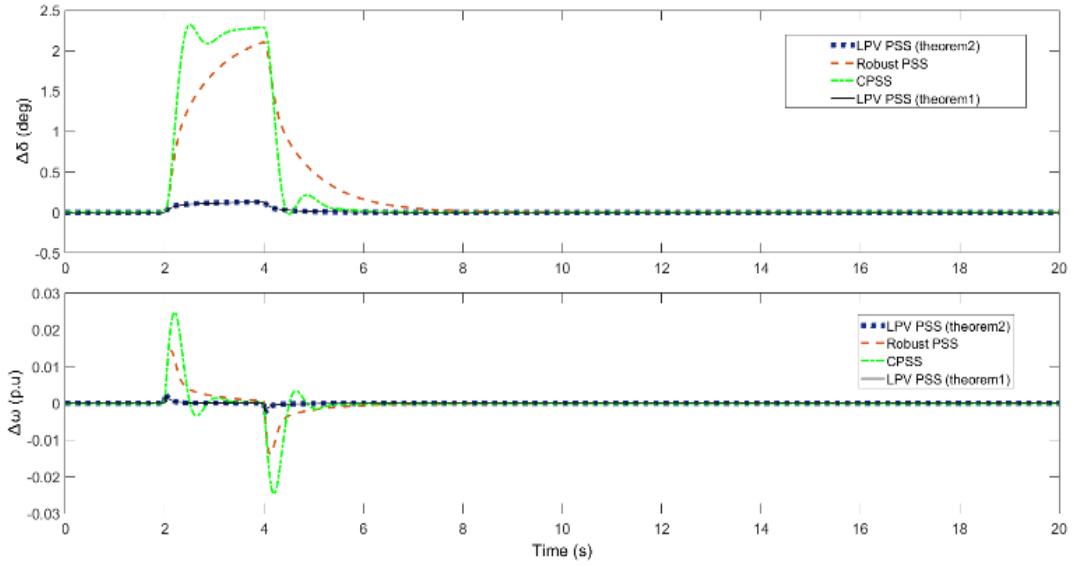

Figure 4. Comparison of LPV PSS, Robust PSS, and CPSS for the first working mode and a sudden change t = 2 s in the input mechanical torque

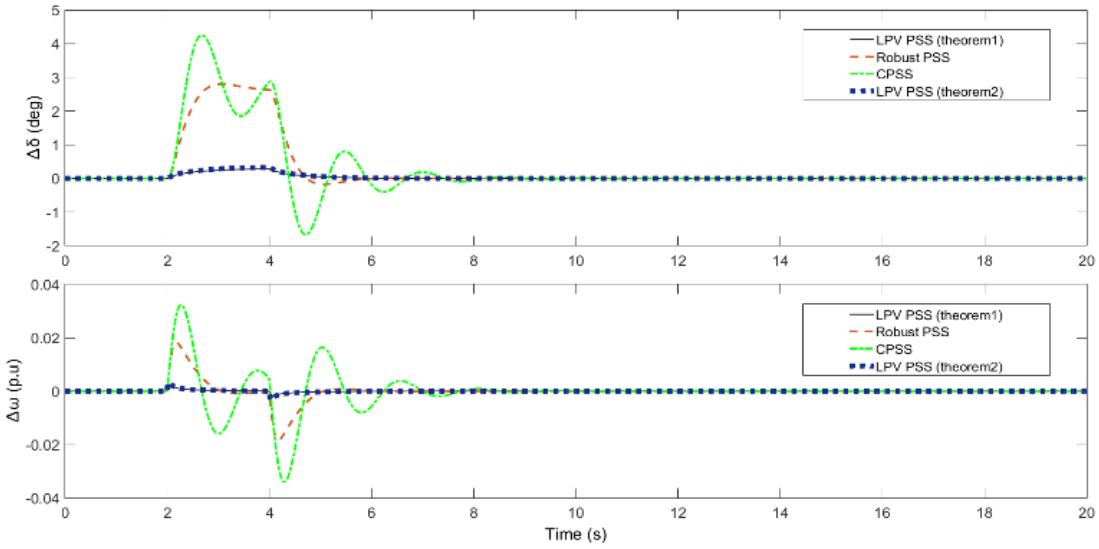

Figure 5. Comparison of LPV PSS, Robust PSS, and CPSS for the second working mode and a sudden change t = 2 s in the input mechanical torque

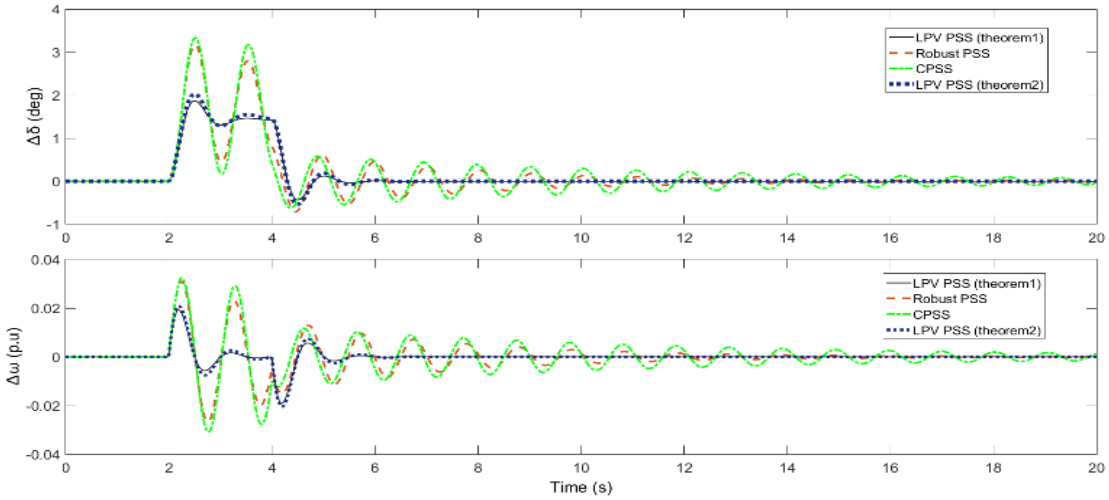

Figure 6. Comparison of LPV PSS, Robust PSS, and CPSS for the third working mode and a sudden change t = 2 s in the input mechanical torque

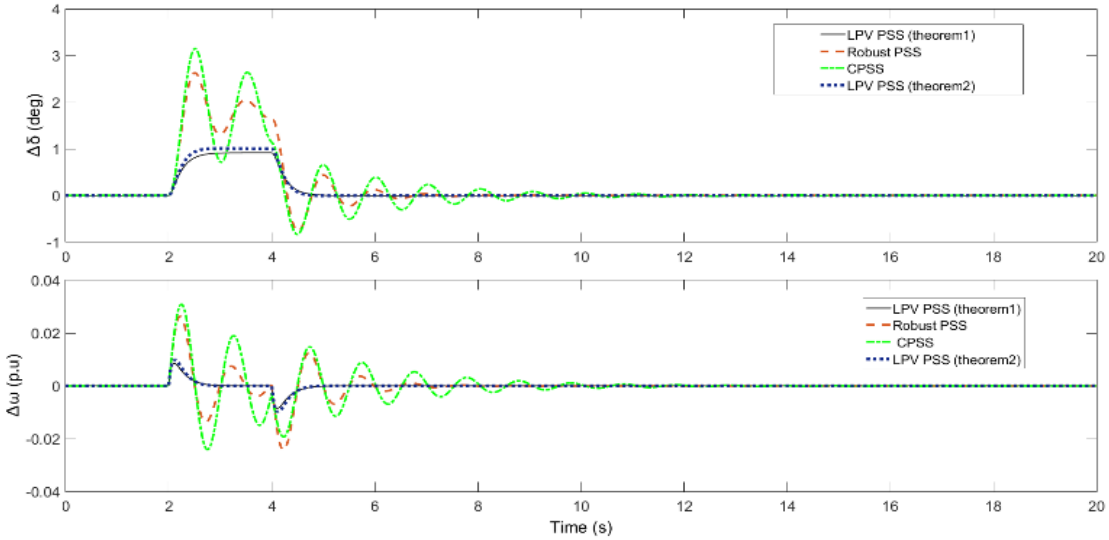

Figure 7. Comparison of LPV PSS, Robust PSS, and CPSS for the fourth working mode and a sudden change t = 2 s in the input mechanical torque

Figures 4-7 show comparisons between LPV controllers from Theories 1 and 2 as well as between the robust PSS and the classic PSS at the mentioned working points with changes in mechanical torque at t = 2 s. It can be observed that Theories 1 and 2 represent better performance in speed and load angle tracking after applying the disturbance and exhibit minmum deviation from the reference values. It should also be noted that the amplitude of overshoots and undershoots in the LPV controllers is much more limited than other control theorems, which is more desirable.

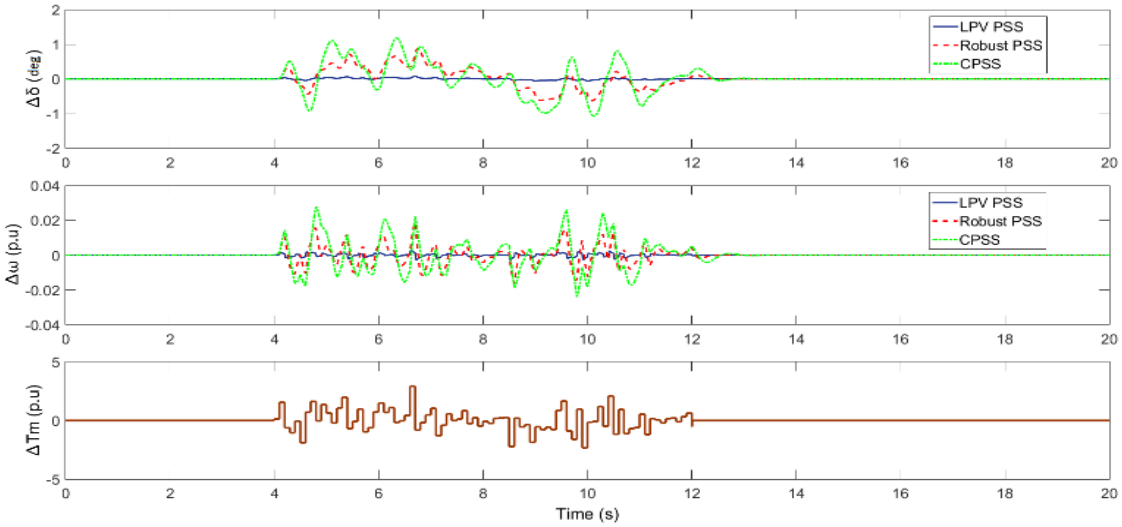

Figure 8. Comparison of LPV PSS, Robust PSS, and CPSS for the first working mode upon applying noise in the input mechanical torque

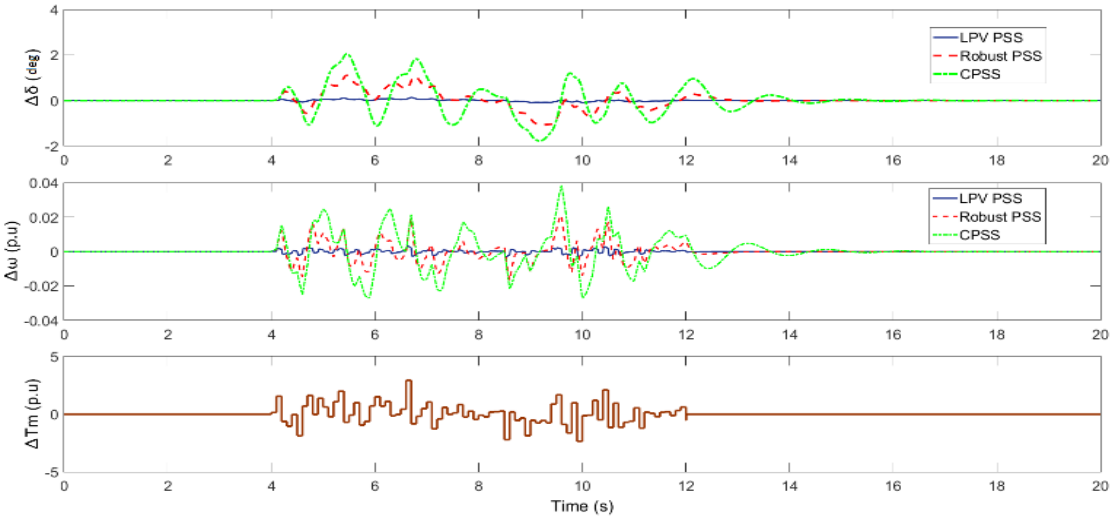

Figure 9. Comparison of LPV PSS, Robust PSS, and CPSS for the second working mode upon applying noise in the input mechanical torque

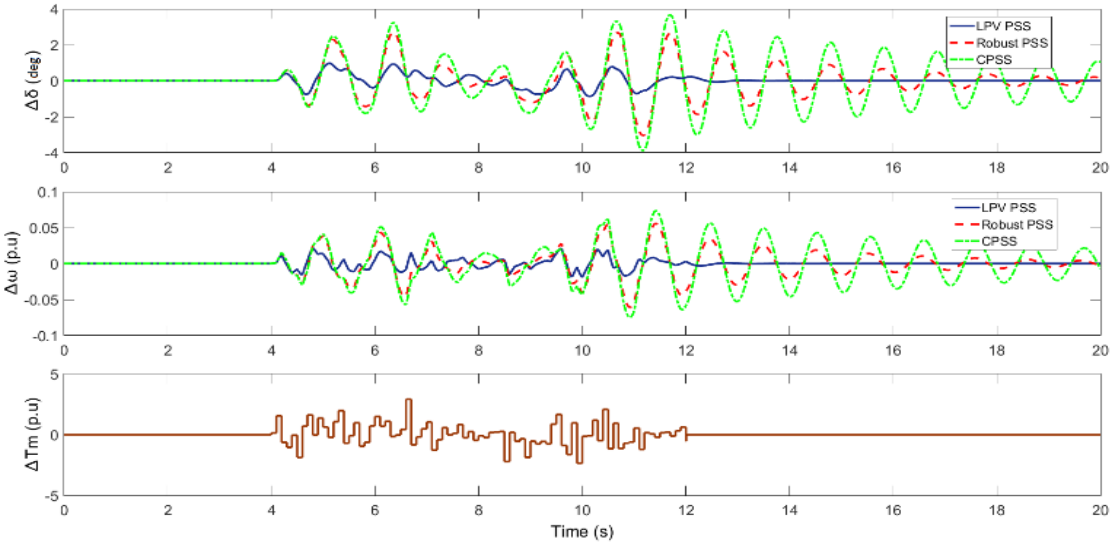

Figure 10. Comparison of LPV PSS, Robust PSS, and CPSS for the third working mode upon applying noise in the input mechanical torque

The variations in load angle, velocity, and mechanical torque in the presence of white noise are shown in Figures 8-10 for three operating points. As illustrated earlier, the proposed LPV controller senses much less perturbations than robust PSS and CPSS. In addition, it is crystal clear that the application of noise in robust and classic PSS creates instability for some operating points and makes $\Delta\delta$ and $\Delta\omega$ oscillate around the reference value. This verifes the incredible performance of the proposed LPV controller.

Now, using Theorem 3 in Section 2.2.2, the Liapanov function is considered as the dependent parameter and the system dynamics is relatively slow. The simulation results are shown in Figures 11-14.

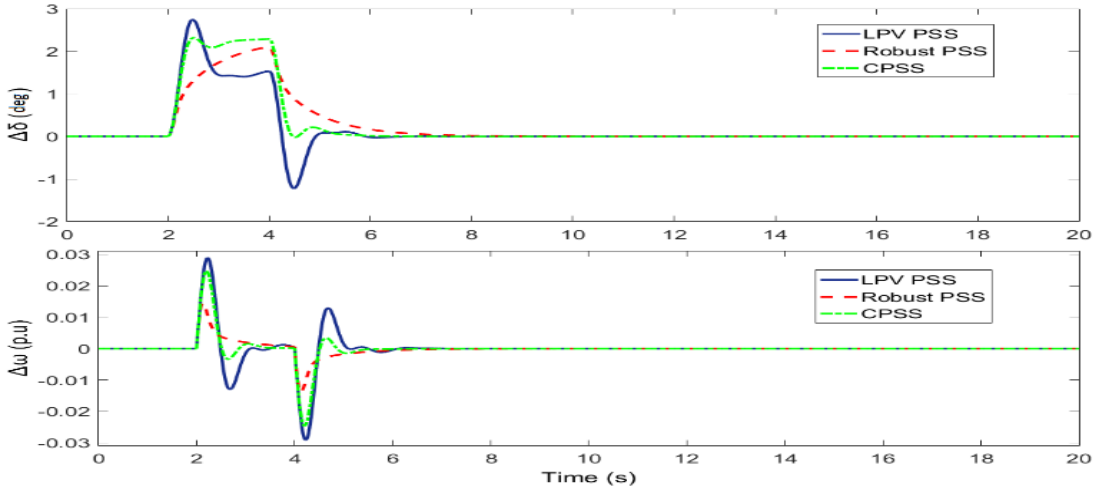

Figure 11. Comparison of LPV PSS, robust PSS, and CPSS for the first working mode and a sudden change t = 2 s in the input mechanical torque

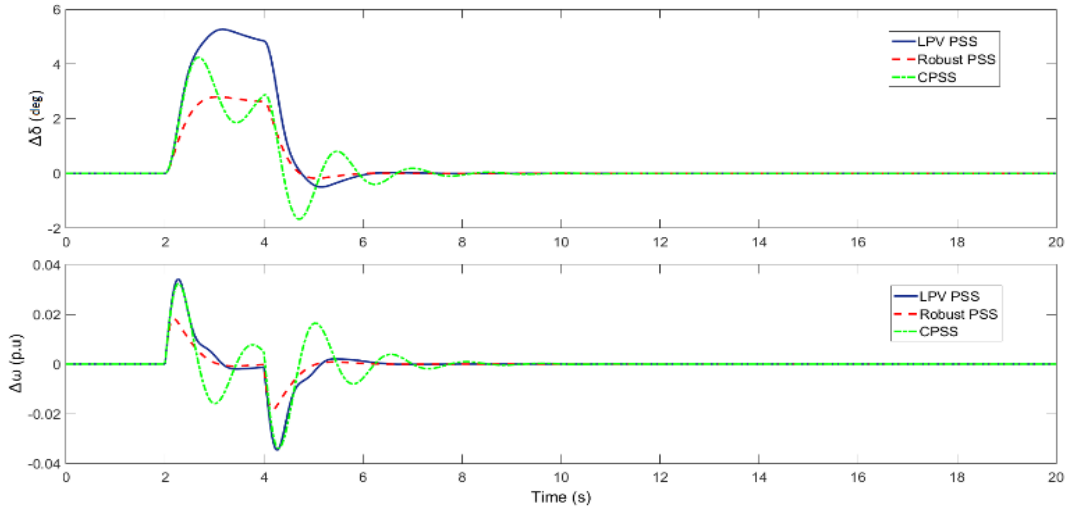

Figure 12. Comparison of LPV PSS, robust PSS, and CPSS for the second working mode and a sudden change t = 2 s in the input mechanical torque

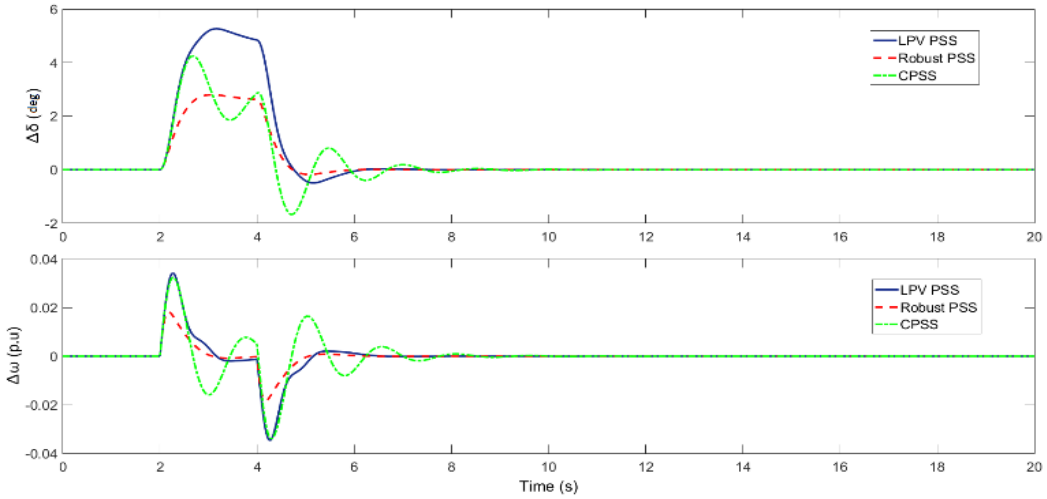

Figure 13. Comparison of LPV PSS, robust PSS, and CPSS for the third working mode and a sudden change t = 2 s in the input mechanical torque

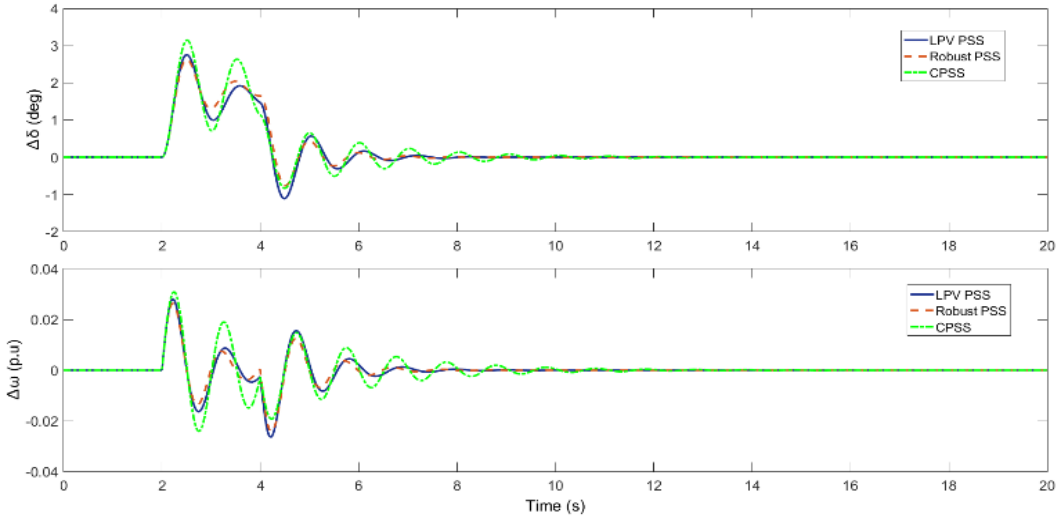

Figure 14. Comparison of LPV PSS, Robust PSS, and CPSS for the fourth working mode and a sudden change t = 2 s in the input mechanical torque

According to Figures 11 to 14, the performance of the LPV controller designed based on Theorem 3 with the proposed polytopic approach by assuming that the variation rate of exogenous parameters is slow (slow dynamic) is not as favorable as it should be and it is less valuable than robust and classic controllers. If Figures 4 to 10 are taken into account, it can be seen that the simulation results based on Theorems 1 and 2 are much more effective than robust and classic methods.

Table 2. Norm comparison in output feedback method related to Theorems 1, 2, and 3

PSS designing method	Largest closed-loop norm (γ_∞)	Iteration	l
Robust	0.023	25	-----
LPV (Theorem 1)	(0.236,0.234,0.228,0.205)	(1,2,3,4)	(0.01,0.001,0.00005,0.00001)
LPV (Theorem 2)	(4.18,2.38,1.115,0.797)	(1,2,3,4)	(0.01,0.005,0.0005,0.00005)
LPV (Theorem 3)	0.267	1	-----

By comparing the best design methods (based on Theorems 1 and 2-Liapanov's fixed function) in Section (2.2.1) and since these controllers are proper and strictly proper respectively, it can be concluded that the controller originated from Theorem 1 has a better performance than Theorem 2.

4.2. State feedback structure

Here, Theorem 4 in Section (2.3) for System (29) with 32-corner polytopes corresponding to the parameters:

$P \in [P^-, P^+]$, $Q \in [Q^-, Q^+]$and $x_e \in [x_e^-, x_e^+]$

$$\begin{cases} k_1 \in [k_1^-, k_1^+] \\ k_2 \in [k_2^-, k_2^+] \\ k_{3i} \in [k_{3i}^-, k_{3i}^+] \\ k_5 \in [k_5^-, k_5^+] \\ k_6 \in [k_6^-, k_6^+] \end{cases}$$

are employed and the state feedback controller gain is obtained.

The following are the simulation results of the stabilizer tuned by the state feedback technique according to Theorem 4 in Section (2.3.) and the output feedback technique in Theorem 1 in Section (2.2.1.). Figures 17-20 demonestrate the simulation results of the comparison of LPV PSS performance in output feedback and state feedback approaches.

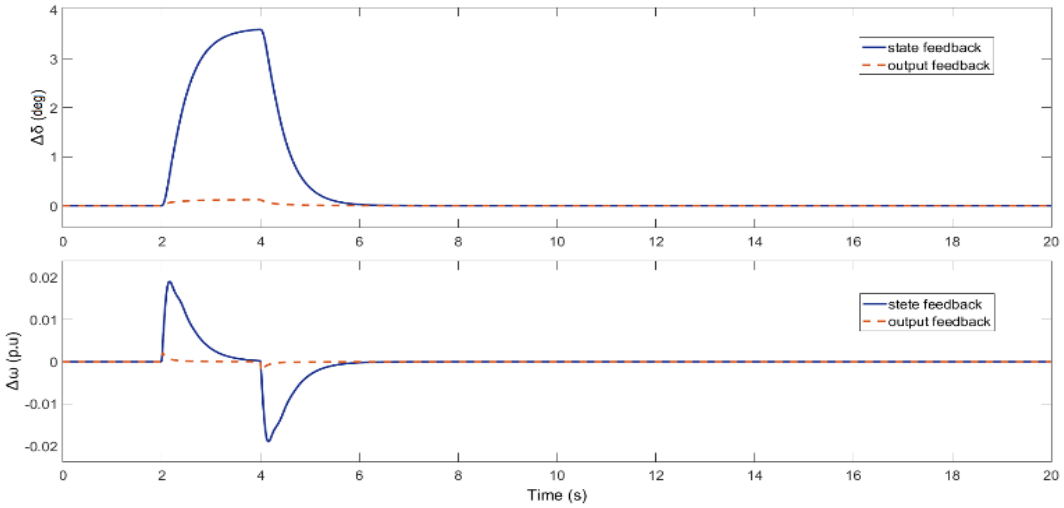

Figure 15. Comparison of LPV PSS performance in output feedback and state feedback methods for the first working mode and a sudden change t = 2 s in input mechanical torque

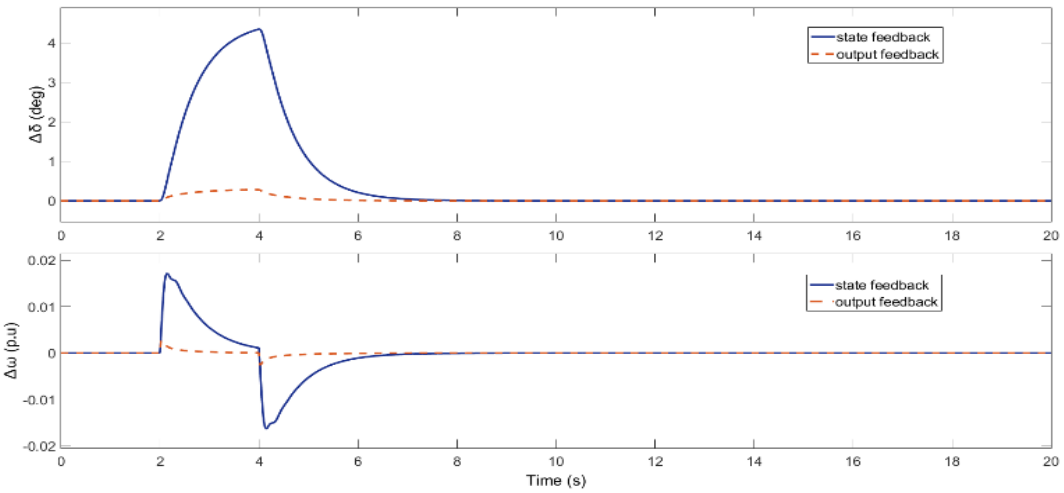

Figure 16. Comparison of LPV PSS performance in output feedback and state feedback methods for the second working mode and a sudden change t = 2 s in input mechanical torque

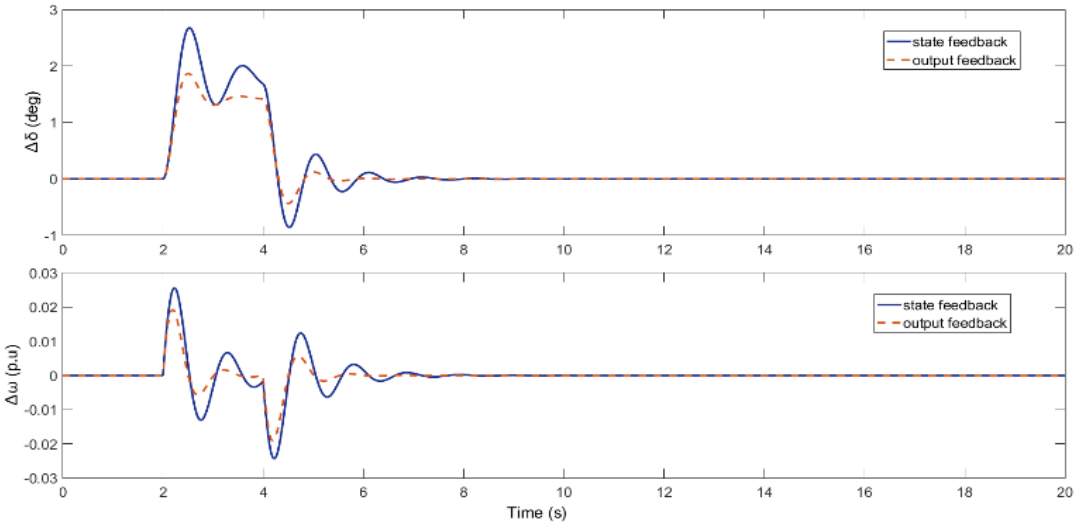

Figure 17. Comparison of LPV PSS performance in output feedback and state feedback methods for the third working mode and a sudden change t = 2 s in input mechanical torque

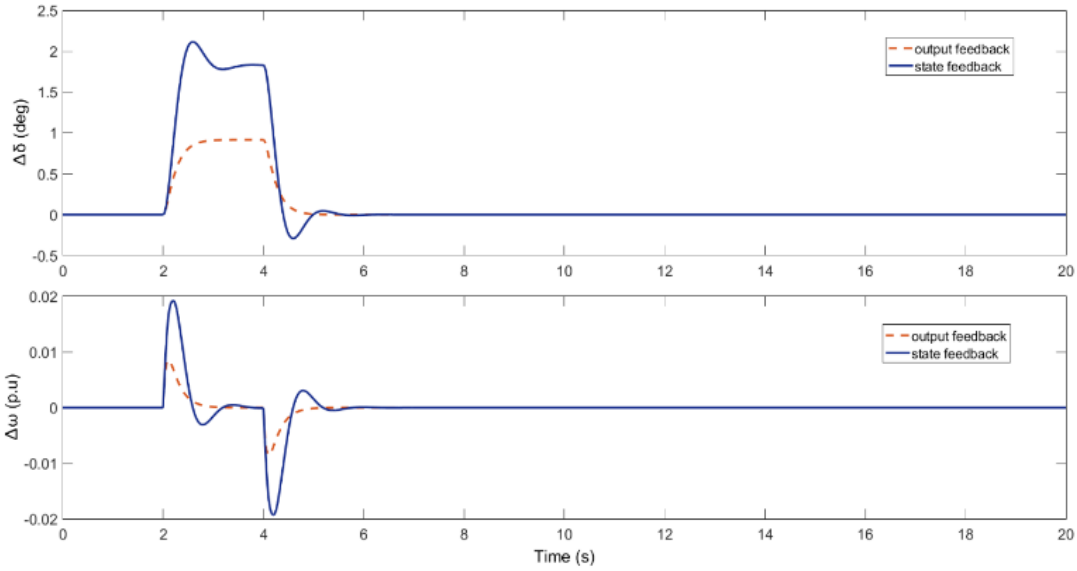

Figure 18. Comparison of LPV PSS performance in output feedback and state feedback methods for the fourth working mode and a sudden change t = 2 s in input mechanical torque

According to Figures 15-18, output feedback design works more presciely than state feedback design to damp the disturbances and minimize the errors. The range of overshoots and undershoots indicates that the proposed LPV PSS designed by output feedback theory is less affected by disturbances.

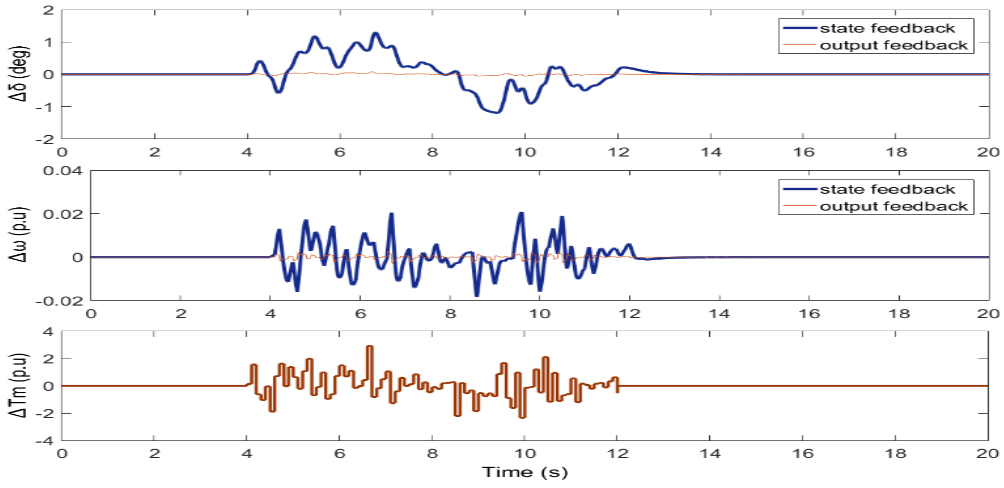

Figure 19. Comparison of LPV PSS performance in output feedback and state feedback methods for the first working mode upon applying noise in the input mechanical torque

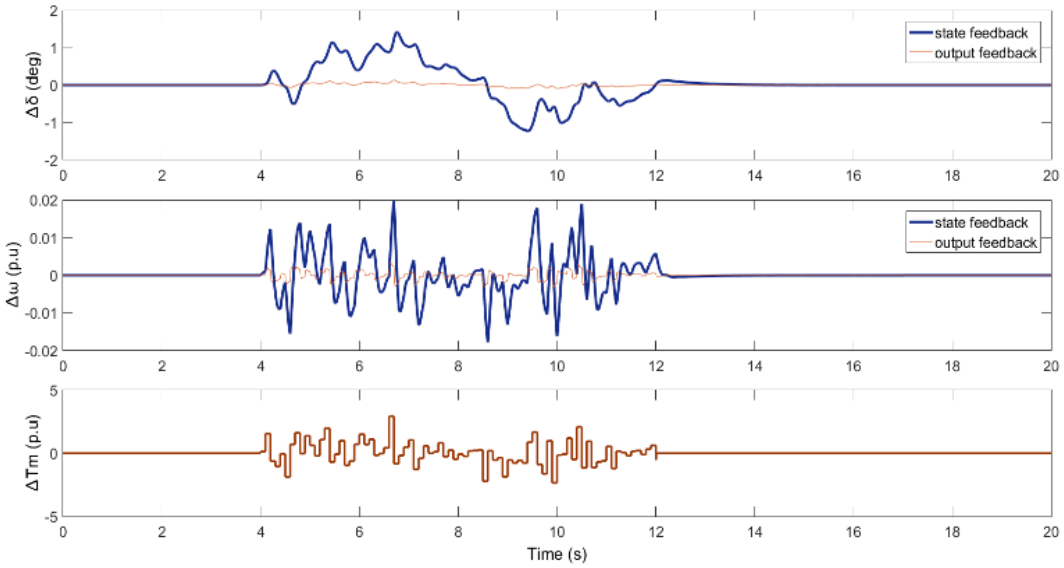

Figure 20. Comparison of LPV PSS performance in output feedback and state feedback methods for the second working mode upon applying noise in the input mechanical torque

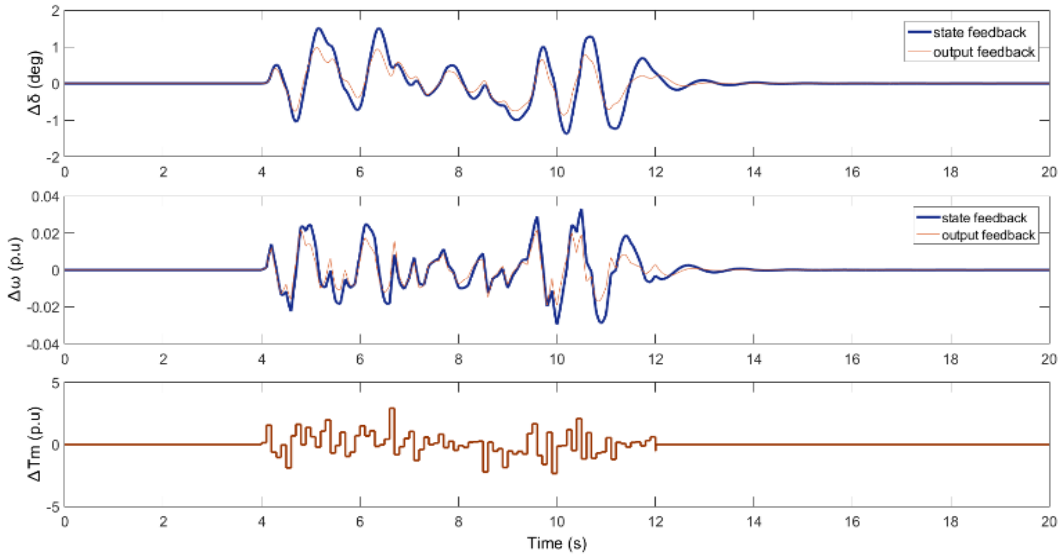

Figure 21. Comparison of LPV PSS performance in output feedback and state feedback methods for the third working mode upon applying noise in the input mechanical torque

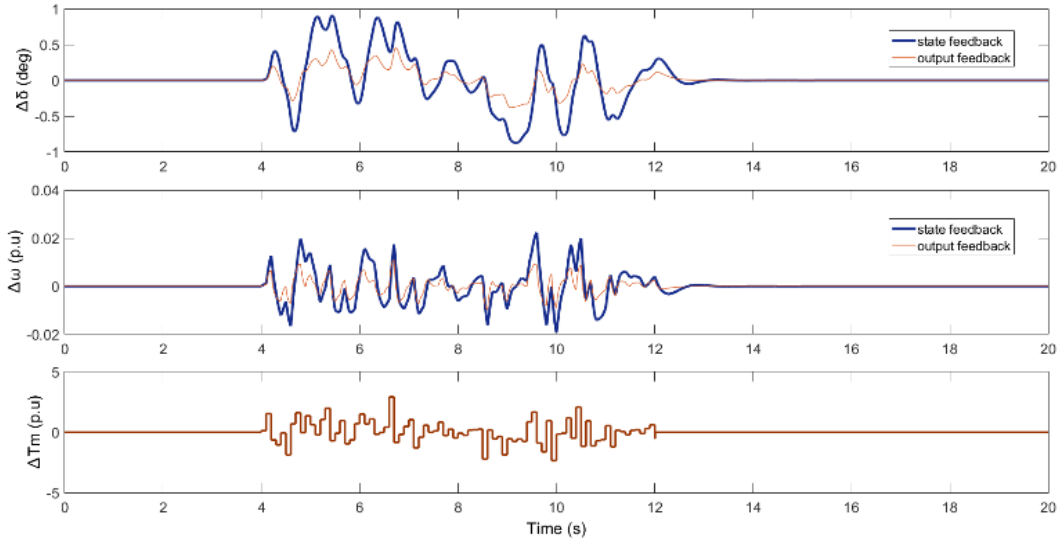

Figure 22. Comparison of LPV PSS performance in output feedback and state feedback methods for the fourth working mode upon applying noise in the input mechanical torque

According to the results derived from Figures 19-22, while noise is applied to the input mechanical torque, the state feedback control system performs weaker than the output feedback one. For a fair comparison, maximum error rates and for two scenarios and four operating points are denoted, as given in Figure 23-26.

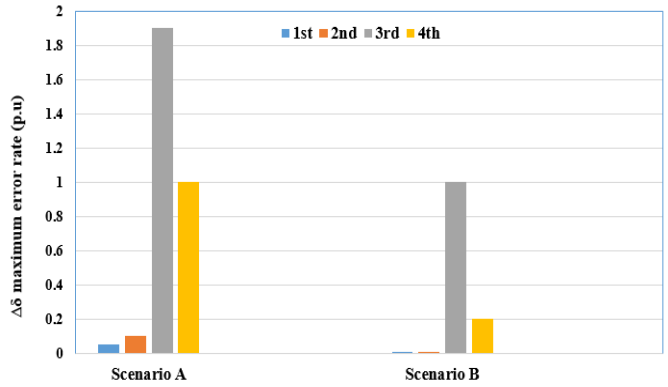

Figure 23. Maximum error rate-output feedback approach tested at four working points. Scenario A: Sudden change in input mechanical torque. Scenario B: Applying noise to input mechanical torque

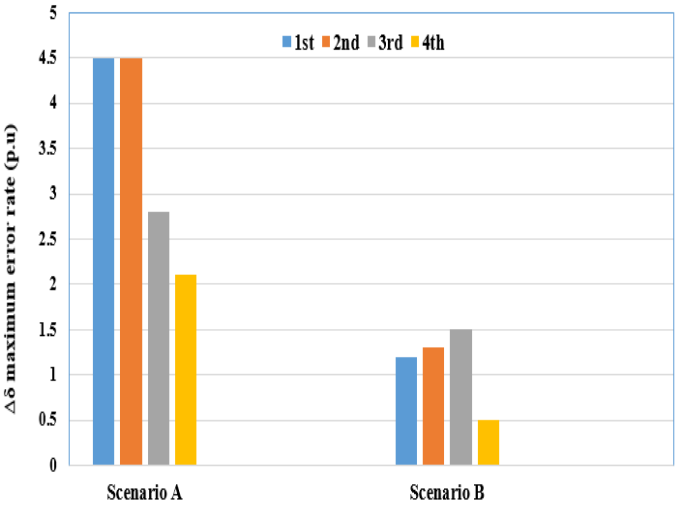

Figure 24. Maximum error rate-state feedback approach tested at 4 working points. Scenario A: Sudden change in input mechanical torque. Scenario B: Applying noise to input mechanical torque

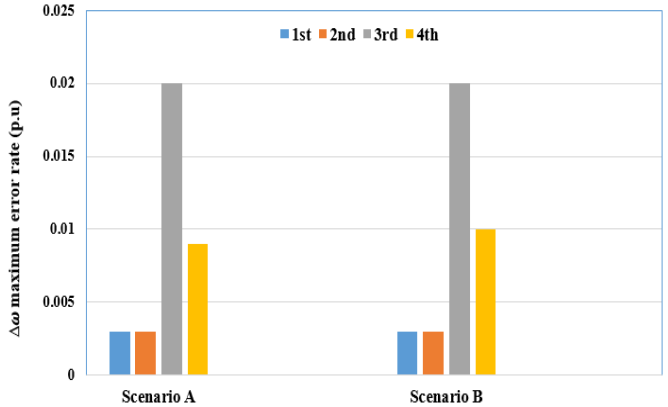

Figure 25. Maximum error rate-output feedback approach tested at 4 working points. Scenario A: Sudden change in input mechanical torque. Scenario B: Applying noise to input mechanical torque

…As can be concluded from the bar charts above, the output feedback theory while applying Scenario A for Δδ has an accurate performance to track reference value and the maximum error rate is 1.9. On the other hand, based on the state feedback theory, the maximum error rate is 4.5, which is much higher than the output feedback approach. Similarly, the rotor angle maximum error rate for the output and state feedback theories are 1 and 1.5, respectively.

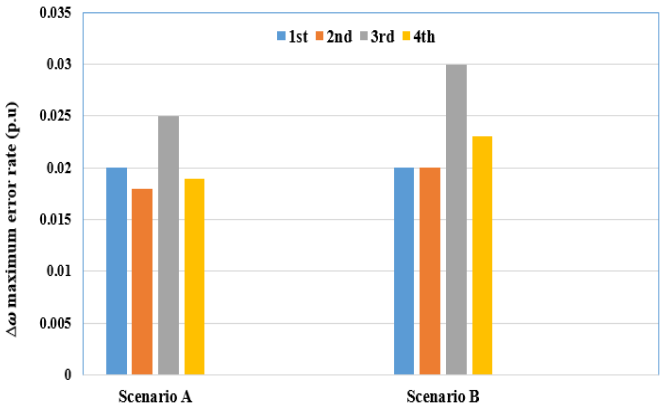

Figure 26. Maximum error rate- state feedback approach tested in 4 working points. Scenario A: Sudden change in input mechanical torque. Scenario B: Applying noise to input mechanical torque

Considering Δω graphs, it is evident that the maximum error rate for both state feedback and output feedback theories is almost the same between 0.02 and 0.03 p.u. Overall, it can be said that the PSS implemented via output feedback theory outweighs the state feedback approach.

Table 3. Norm comparison in output feedback and state feedback methods for Theorems 1 and 4

Largest closed-loop norm	Desired theorems
$\gamma_{\infty}=0.267$	Theorem 1 (Output feedback)
$\gamma_{\infty}=0.063$	Theorem 4 (State feedback)

In this paper, Matlab Software was used for the aim of simulation. The convergence time depends the order of generator model and on the polytope vertices. The higher the order of the system, the more complex the controller design and the longer the convergence time.

The proposed strategy flowchart is finally presented here for clarifying the overall methodolgy.

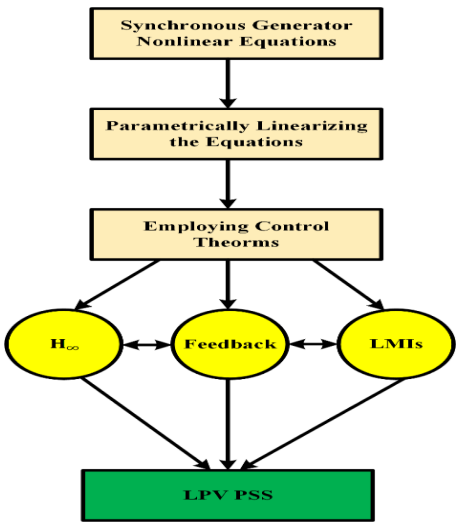

Figure 27. Overall proposed control strategy flowchart

5. CONCLUSIONS

Low frequency oscillations in interconnected power systems are considered as the main challenge. This paper suggests a control strategy based on LPV method to obtain an effective power system stabilizer rejecting noises and disturbances. This system was examined by applying different inputs as well as different operating conditions of the proposed stabilizing performance. Also, the effectiveness of the proposed controller design was compared to the robust and classic design considering the uncertainties of the model and changes in the working conditions. Polytopic representation and LMI optimization are employed to design output feedback and state feedback controllers in order to create a power system stabilizer. Upon comparing the proposed methods and controllers, it was found that PSS designed via LPV method and based on output feedback theory provided better results. In addition, good stability and damping over the whole range of system conditions are guaranteed. This designed PSS can be utilized in intertwined power systems including renewable units to suppress the oscillations.

6. ACKNOWLEDGEMENT

This research did not receive any specific grant from funding agencies in the public, commercial, or not-for-profit sectors.

NOMENCLATURE

P	Active power (w)
Q	Reactive power (var)
Xe	External reactance of transmission line (Ω)
$k_1 \dots k_6$	PSS fourth-order model constants
u	Stabilizer output
w	Disturbance input
y	Measured output
$\Delta\omega$	Velocity deviation (rad/s)
$\Delta\delta$	Load angle deviation
ΔE_q	Electromagnetic force deviation (kg. m/s^2)
ΔE_{fd}	Generator field excitation voltage deviation (v)
T_E	Exciter time constant (s)
K_E	Exciter gain
T'_{d0}	Open circuit field time constant (s)
M	Inertia constant (s)
D	Damping coefficient
x_d	d-axis transient reactance (Ω)
x_q	q-axis transient reactance (Ω)
x'_d	d-axis synchronous reactance (Ω)
K_s	PSS gain
T_w	Washout time constant (s)
$T_1 \dots T_4$	Time constant of lead compensator (s)

APPENDICES

Appendix A: System parameters

Parameter	Value
V	1 p.u
ω_0	314 rpm
M	10 s
x'_d	0.32 p.u
x_d	1.6 p.u
x_q	1.55 p.u
K_E	25
T_E	0.05 s
T'_{d0}	6 s
D	0.05 p.u

Appendix B: Calculation of k_1 to k_6

$$C_1 = \frac{V^2}{x_e + x_q}, \qquad C_3 = C_1 \frac{x_q - x'_d}{x_e + x'_d}, \qquad C_4 = \frac{V}{x_e + x'_d}$$

$$C_5 = V \frac{x_d - x'_d}{x_e + x'_d}, \qquad C_6 = C_1 \frac{x_q (x_q - x'_d)}{x_e + x'_d}, \qquad C_7 = \frac{x_e}{x_e + x'_d}$$

$$k_1 = C_3 \frac{P}{P^2 + (Q + C_1)^2} + Q + C_1$$

$$k_2 = C_4 \frac{P^2}{\sqrt{P^2 + (Q + C_1)^2}}, \qquad k_3 = \frac{x_e + x'_d}{x_d + x'_d}$$

$$k_4 = C_5 \frac{P^2}{\sqrt{P^2 + (Q + C_1)^2}}$$

$$k_5 = C_4 x_e \frac{P}{V^2 + Q x_e} \left[C_6 \frac{C_1 + Q}{P^2 + (C_1 + Q)^2} - x'_d \right]$$

$$k_6 = C_7 \frac{\sqrt{P^2 + (Q + C_1)^2}}{V^2 + Q x_e} \left[x_e + \frac{C_1 x_q (C_1 + x_q)}{P^2 + (C_1 + Q)^2} \right]$$

REFERENCES

1. Kundur, P., Balu, N.J. and Lauby, M.G., Power system stability and control, Vol. 7, McGraw-Hill, New York, (1994). (http://www.elcom-hu.com/Electrical/Power%20System%20Stability/%5Bprabha%20kundur%5D%20powr%20system%20stability%20and%20control.pdf).
2. Wang, S.K., "Coordinated parameter design of power system stabilizers and static synchronous compensator using gradual hybrid differential evaluation", ***International Journal of Electrical Power & Energy Systems***, Vol. 81, (2016), 165-174. (https://doi.org/10.1016/j.ijepes.2016.02.016).
3. Dey, P., Bhattacharya, A. and Das, P., "Tuning of power system stabilizer for small signal stability improvement of interconnected power system", ***Applied Computing and Informatics***, Vol. 16, (2017), 3-28. (https://doi.org/10.1016/j.aci.2017.12.004).
4. Jin, T., Liu, S., Flesch, R.C. and Su, W., "A method for the identification of low frequency oscillation modes in power systems subjected to noise", ***Applied Energy***, Vol. 206, (2017), 1379-1392. (https://doi.org/10.1016/j.apenergy.2017.09.123).
5. Eltag, K., Aslamx, M.S. and Ullah, R., "Dynamic stability enhancement using fuzzy PID control technology for power system", ***International Journal of Control, Automation and Systems***, Vol. 1, (2019), 234-242. (https://doi.org/10.1007/s12555-018-0109-7).
6. Suzuki, K., Kobayashi, J., Otani, T. and Iwamoto, S., "A multi-input lead-lag power system stabilizer with H_∞ control performance", ***Proceedings of 2015 IEEE Innovative Smart Grid Technologies-Asia (ISGT ASIA)***, (2015), 1-6. (https://doi.org/10.1109/ISGT-Asia.2015.7387023).
7. Abido, M.A., "A novel approach to conventional power system stabilizer design using tabu search", ***International Journal of Electrical Power & Energy Systems***, Vol. 2, (1999), 443-454. (https://doi.org/10.1016/S0142-0615 (99)00004-6).
8. Farahani, M. and Ganjefar, S., "Intelligent power system stabilizer design using adaptive fuzzy sliding mode controller", ***Neurocomputing***, Vol. 226, (2017), 135-144. (https://doi.org/10.1016/j.neucom.2016.11.043).
9. Bouchama, Z. and Harmas, M.N., "Optimal robust adaptive fuzzy synergetic power system stabilizer design", ***Electric Power Systems Research***, Vol. 83, (2012), 170-175. (https://doi.org/10.1016/j.epsr.2011.11.003).
10. Guesmi, T. and Alshammari, B.M., "An improved artificial bee colony algorithm for robust design of power system stabilizers", ***Engineering Computations***, Vol. 34, (2017), 2131-2153. (https://doi.org/10.1108/EC-12-2016-0459).

11. Sambariya, D.K. and Prasad, R., "Robust power system stabilizer design for single machine infinite bus system with different membership functions for fuzzy logic controller", ***Proceedings of 7th International Conference on Intelligent Systems and Control (ISCO)***, (2013). (https://doi.org/10.1109/ISCO.2013.6481115).
12. Milla, F. and Duarte-Mermoud, M.A., "Predictive optimized adaptive PSS in a single machine infinite bus", ***ISA Transactions***, Vol. 63, (2016), 315-327. (https://doi.org/10.1016/j.isatra.2016.02.018).
13. Farhad, Z., Eke, H., Tezcan, S. and Safi, S., "A robust PID power system stabilizer design of single machine infinite bus system using firefly algorithm", ***Gazi University Journal of Science***, Vol. 31, (2018), 155-172. (https://dergipark.org.tr/en/pub/gujs/issue/35772/346118).
14. Khawaja, A.W., Kamari, N.A.M. and Zainuri, M.A.A.M., "Design of a damping controller using the SCA optimization technique for the improvement of small signal stability of a single machine connected to an infinite bus system", ***Energies***, Vol. 14, (2021). (https://doi.org/10.3390/en14112996).
15. Kadir, N. and Ruswandi Djalal, M., "Optimal design PSS-PID control on single machine infinite bus using ANT COLONY optimization", ***SINERGI***, Vol. 25, (2021), 169-176. (http://doi.org/10.22441/sinergi.2021.2.008).
16. Bolinger, K., Laha, A., Hamilton, R. and Harras, T., "Power stabilizer design using root locus methods", ***IEEE Transactions on Power Apparatus and Systems***, Vol. 94, (1975), 1484-1488. (https://doi.org/10.1109/T-PAS.1975.31990).
17. Gibbard, M.J., "Robust design of fixed-parameter power system stabilizers over a wide range of operating conditions", ***IEEE Transactions on Power Apparatus and Systems***, Vol. 6, (1991), 794-800. (https://doi.org/10.1109/59.76727).
18. Abido, M.A., "Optimal design of power-system stabilizers using particle swarm optimization", ***IEEE Transactions on Energy Conversion***, Vol. 17, (2002), 406-413. (https://doi.org/10.1109/TEC.2002.801992).
19. Bandal, V. and Bandyopadhyay, B., "Robust decentralised output feedback sliding mode control technique-based power system stabilizer (PSS) for multimachine power system", ***IET Control Theory Applications***, Vol. 1, (2007), 1512-1522. (https://doi.org10.1049/iet-cta:20060393).
20. El-Metwally, K.A., "An adaptive fuzzy logic controller for a two area load frequency control problem", ***Proceedings of 12th International Middle-East Power System Conference***, (2008), 300-306. (https://doi.org/10.1109/MEPCON.2008.4562327).
21. Shakarami, M.R. and Davoudkhani, I.F., "Wide-area power system stabilizer design based on grey wolf optimization algorithm considering the time delay", ***Electric Power Systems Research***, Vol. 133, (2016), 149-159. (https://doi.org/10.1016/j.epsr.2015.12.019).
22. Hemmati, R., "Power system stabilizer design based on optimal model reference adaptive system", ***Ain Shams Engineering Journal***, Vol. 9, (2018), 311-318. (https://doi.org/10.1016/j.asej.2016.03.002).
23. Kashani, M., Alfi, A. and Arabkoohsar, A., "Optimal robust control scheme to enhance power system oscillations damping via STATCOM", ***Proceedings of 2020 International Conference on Smart Energy Systems and Technologies (SEST)***, (2020), 1-6. (https://doi.org/10.1109/SEST48500.2020.9203361).
24. Guesmi, T., Farah, A., Abdallah, H.H. and Ouali, A., "Robust design of multi-machine power system stabilizers based on improved non-dominated sorting genetic algorithms", ***Electrical Engineering***, Vol. 100, (2018), 1351-1363. (https://doi.org/10.1007/s00202-017-0589-0).
25. Nogueira, F.G., Barra Jr, W., da Costa Jr, C.T., Barreiros, J.A. and de Lana, J.J., "Design and experimental tests of an LPV power system stabilizer on a 10kVA small-scale generating unit", ***IFAC-PapersOnLine***, Vol. 48, (2015), 236-241. (https://doi.org/10.1016/j.ifacol.2015.11.143).
26. Jabali, M.B.A. and Kazemi, M.H., "A new LPV modeling approach using PCA-based parameter set mapping to design a PSS", ***Journal of Advanced Research***, Vol. 8, (2017), 23-32. (https://doi.org/10.1016/j.jare.2016.10.006).
27. Shamma, J.S., "An overview of LPV system",Control of linear parameter varying systems with applications,Mohammadpour, J. and Scherer, C. eds., Springer, Boston, MA, (2012), 3-26. (https://doi.org/10.1007/978-1-4614-1833-7_1).
28. Bruzelius, F., "An approach to gain scheduling linear parameter varying system", ***Chalmers University of Technology***, (2004). (https://elibrary.ru/item.asp?id=8860385).
29. Sato, M. and Peaucelle, D., "Gain-scheduled output-feedback controllers using inexact scheduling parameters for continuoustime LPV systems", ***Automatica***, Vol. 49, (2013), 1019-1025. (https://doi.org/10.1016/j.automatica.2013.01.034).
30. Sadeghzadeh, A., "Gain-scheduled filtering for linear parameter-varying systems using inexact scheduling parameters with bounded variation rates", ***International Journal of Robust and Nonlinear Control***, Vol. 26, (2015), 2864-2879. (https://doi.org/10.1002/rnc.3482).
31. Xie, R., Wang, X. and Li, Y., "State feedback control for the stabilization of the three Euler angles of helicopter based on LMI", ***Proceedings of International Conference on Intelligent Computation Technology and Automation***, (2008). (https://doi.org/10.1109/ICICTA.2008.332).
32. Soliman, H.M., Emara, H., Elshafei, A.L., Bahgat, A. and Malik, O.P., "Robust output feedback power system stabilizer design: An LMI approach", ***2008 IEEE Power and Energy Society General Meeting–Conversion and Delivery of Electrical Energy in the 21st Century***, USA, (2008), 1-8. (https://doi.org/10.1109/PES.2008.4596450).
33. Soliman, H.M., Elshafei, A.L., Shaltout. A.A. and Morsi, M.F., "Robust power system stabilizer", ***IEEE Proceedings-Electric Power Applications***, Vol. 147, (2000), 285–291. (https://ieeexplore.ieee.org/document/874989/).
34. Demello, F.P. and Concordia, C., "Concepts of synchronous machine stability as affected by excitation control", ***IEEE Transactions on Power Apparatus and Systems***, Vol. 88, (1969), 316-329. (https://doi.org/10.1109/TPAS.1969.292452).
35. Lofberg, J., "YALMIP: A toolbox for modeling and optimization in MATLAB", ***Proceedings of IEEE International Conference on Robotics and Automation***, (2004). (https://doi.org/10.1109/CACSD.2004.1393890).
36. Agulhari, C.M., De Oliveira, R.C.L.F. and Peres, P.L.D., "Robust LMI parser: A computational package to construct LMI conditions for uncertain systems", ***Proceedings of Brazilian Conference on Automation (CBA 2012)***, Campina Grande, PB, Brazil, (2012), 2298-2305. (https://doi.org/10.1145/3323925).
37. Yang, T.C., "Applying H_∞ optimization method to power system stabilizer design, Part 1: single-machine infinite-bus systems", ***International Journal of Electrical Power & Energy Systems***, Vol. 19, (1997), 29-35. (https://doi.org/10.1016/S0142-0615 (96)00026-9).
38. Demello, F.P. and Concordia, C., "Concepts of synchronous machine stability as affected by excitation control", ***IEEE Transactions on Power Apparatus and Systems***, Vol. 88, (1969), 316-329. (https://doi.org/ 10.1109/TPAS.1969.292452).